Stellar Structure and Evolution
Lab Assignment

Ioannis Koutalios
s3365530

June 16, 2023

1 Introduction

During their lives, stars pass through many different evolutionary stages. The biggest factor in how a star will evolve from a protostar to the final stage of its life greatly depends on its initial mass. In this project, we will simulate the evolution of two stars with masses $1\,M_\odot$ and $2\,M_\odot$ from their birth to model their evolution.

2 Methods

For the numerical simulation of the star evolution, we will use the `MESA` module [1, 2, 3, 4, 5]. The module allows us to define the initial mass of the protostar and model it through all the different stages until it becomes a white dwarf. The results we obtained were analyzed in `Python` using the `PyMesaReader` module [6]. We want to create four plots for each initial mass. The first one is the evolution of the core in the $\log(T_c)$ - $\log(R_c)$ plane. The second one is the evolution of the star in the Hertzburg-Russel diagram. Finally, we want to plot the adiabatic and radiative gradients for the pre-main and main sequence phases as a function of the radius.

3 Results

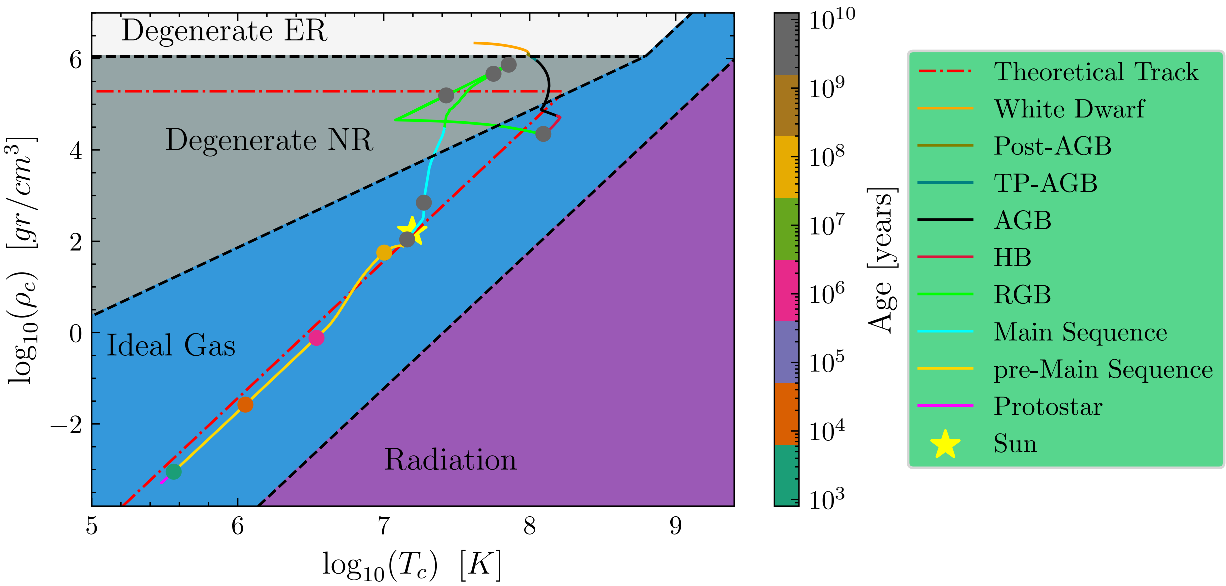

Figure 1: The logarithm of the core density of the star with $M = 1M_\odot$ as a function of the logarithm of the temperature of its core. In the plot, we can see the different regions where each equation of state dominates. The different evolutionary stages of the star are plotted with different colors. The color of the points shows their age. The relative position of the Sun is also depicted.

To study the evolution of the core of the stars we simulated, we plot the density of the core as a function of its temperature. The results for the two stars are shown in Figures 1 and 2. To better visualize the results we plot the four different regions that emerge in this type of diagram depending on the equations of state [7]:

$$P_{gas} = \frac{R}{\mu}T\rho,\ P_e = K_{NR}(\frac{\rho}{\mu_e})^{\frac{5}{3}},\ P_e = K_{ER}(\frac{\rho}{\mu_e})^{\frac{5}{3}},\ P_{rad} = \frac{aT^4}{3} \tag{1}$$

where ρ is the density, T the temperature, R the universal gas constant, μ the mean atomic mass, μ_e the mean atomic mass per electron, and K are the constants for the non-relativistic and extremely relativistic gas.

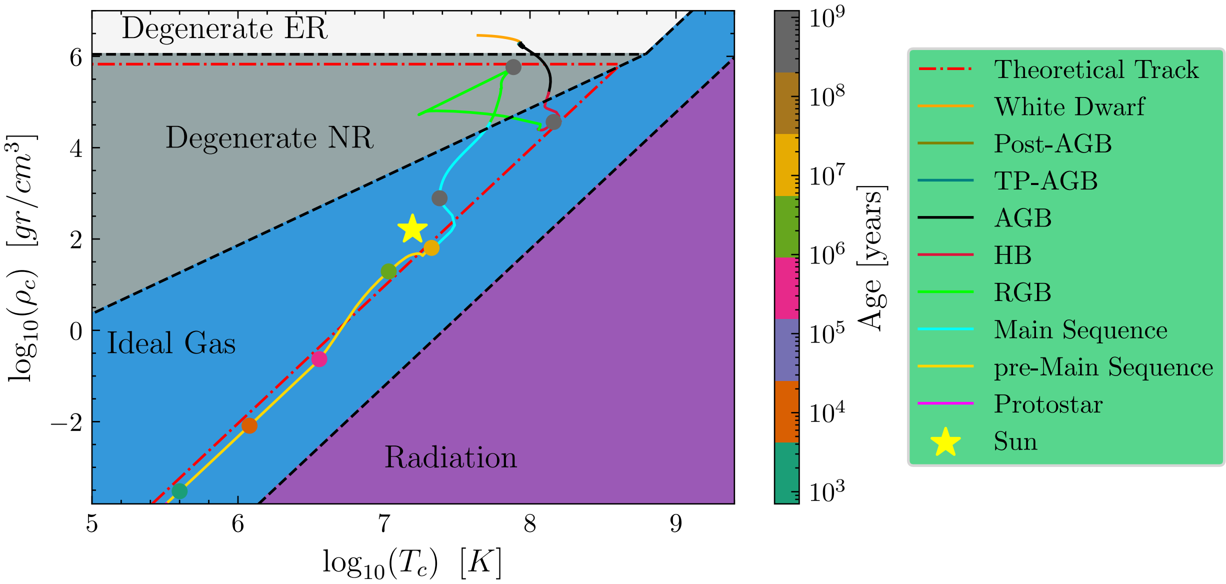

Figure 2: The logarithm of the core density of the star with $M = 2M_\odot$ as a function of the logarithm of the temperature of its core. In the plot, we can see the different regions where each equation of state dominates. The different evolutionary stages of the star are plotted with different colors. The color of the points shows their age. The relative position of the Sun is also depicted.

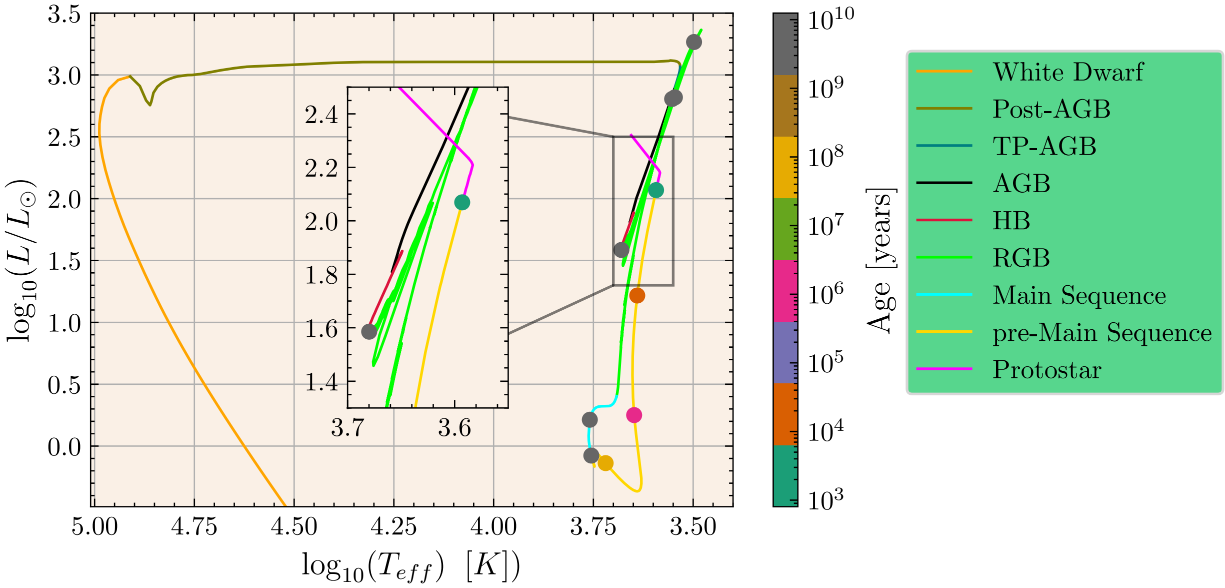

Figure 3: The log Luminosity of the star with $M = 1M_\odot$ as a function of the log of the effective Temperature. The colors of the lines represent the different evolutionary stages and for the dots, we have the different ages of the star. Plots like this are also known as Hertzsprung-Russel diagrams.

The first equation of state is for the ideal gas. The next two equations of state show the non-relativistic and extremely relativistic pressure of the electrons, while the last one is the pressure of the radiation. To find the regions in which each one dominates we can solve for the equality of each pair that arises.

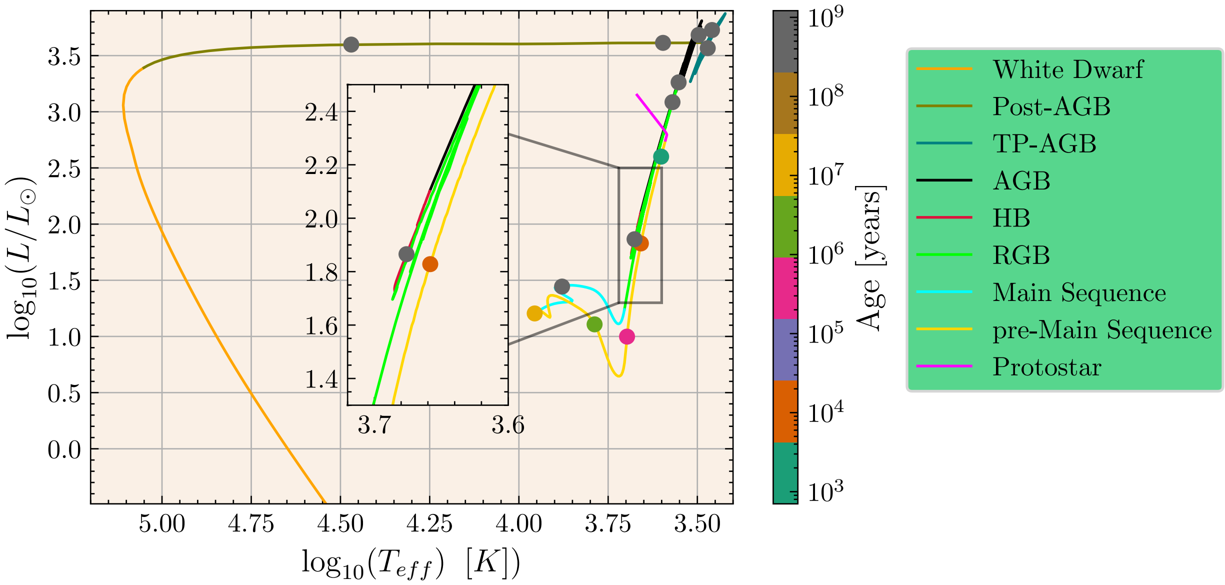

Figure 4: The log Luminosity of the star with $M = 2M_\odot$ as a function of the log of the effective Temperature. The colors of the lines represent the different evolutionary stages and for the dots, we have the different ages of the star. Plots like this are also known as Hertzsprung-Russel diagrams.

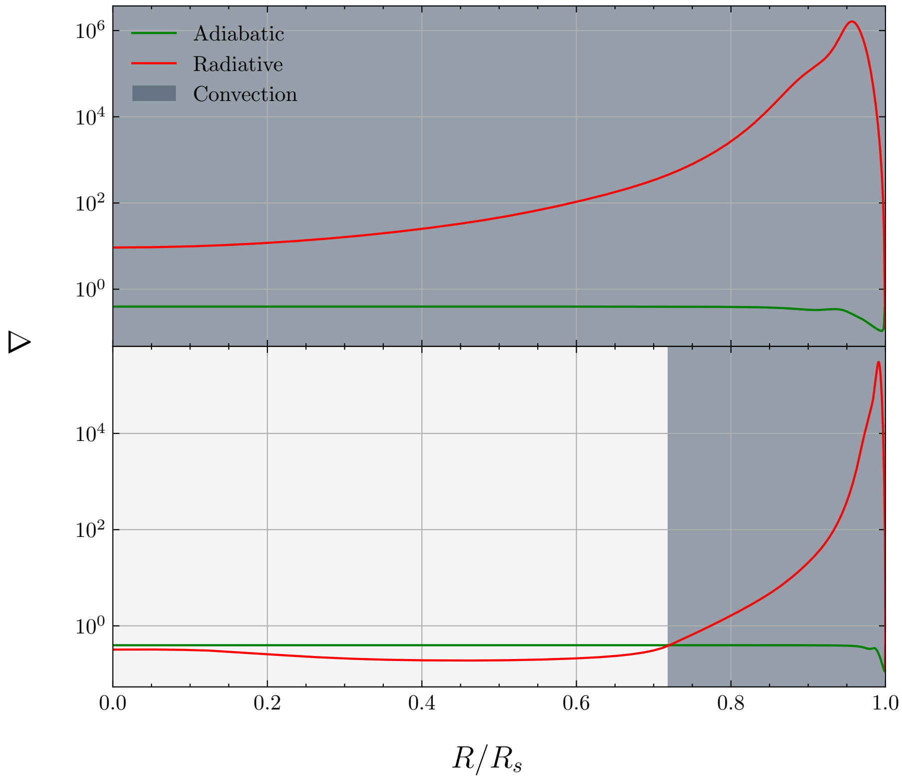

Figure 5: The radiative gradient with the adiabatic one as a function of the relative radius for the star with $M = 1M_\odot$. On the top panel, we have the pre-Main Sequence phase of the star while on the bottom panel, we have the plots for the Main Sequence. The region of convection is also noted on the plot.

To calculate the limits we want to find the regions where the equations of state are equal to each other. The results of these calculations are:

$$\rho = \mu_e^{\frac{5}{2}} (\frac{RT}{\mu K_{NR}})^{\frac{3}{2}} \; [gas - NR], \quad \rho = \mu_e^4 (\frac{RT}{\mu K_{ER}})^3 \; [gas - ER]$$

$$\rho = \frac{a\mu T^3}{3R} \; [gas - rad], \quad \rho = \mu_e (\frac{K_{ER}}{K_{NR}})^3 \; [ER - NR] \tag{2}$$

In Figures 3 and 4 we have the Hertzsprung-Russel (H-R) diagrams for the evolution of the two stars. We plot the logarithm of the star Luminosity as a function of the effective Temperature in a log-log plot. As the star evolves, its location in the H-R diagram changes. The exact evolution of the star greatly depends on its initial mass.

Finally, we create the plots for the adiabatic and radiative gradients as a function of the relative radius. We are interested in two phases of each star's evolution, the pre-Main Sequence and the Main-Sequence. In Figures 5 and 6 we can find both profiles for each star. We also note the regions where convection occurs. The condition for this is when $\nabla_{radiative} > \nabla_{adiabatic}$ which is known as the Schwarzschild criterion for stability against convection.

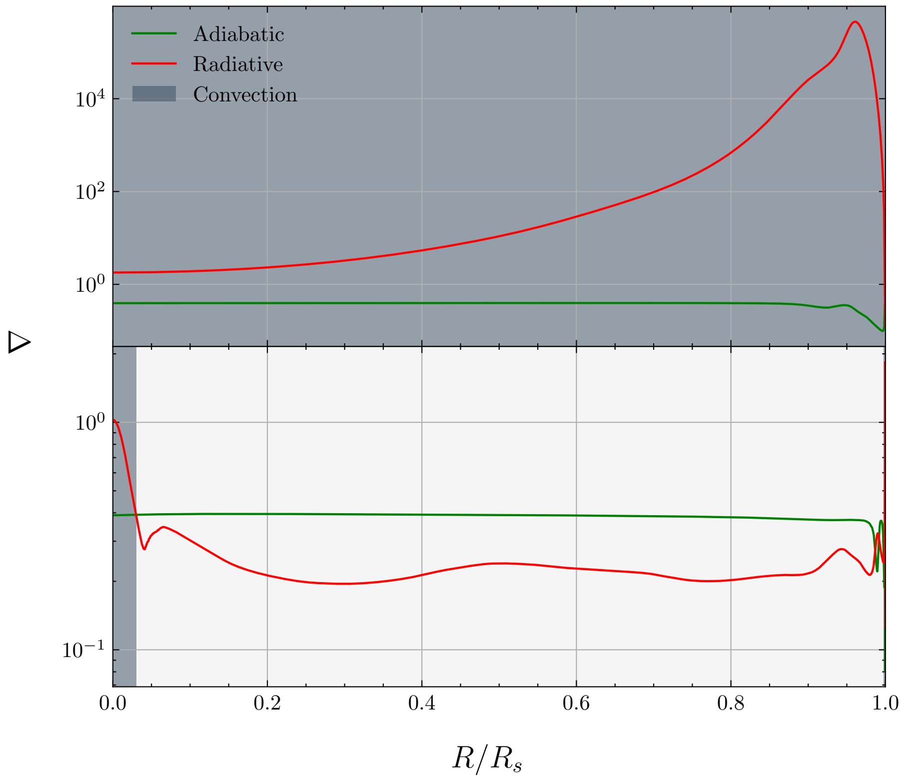

Figure 6: The radiative gradient with the adiabatic one as a function of the relative radius for the star with $M = 2M_{\odot}$. On the top panel, we have the pre-Main Sequence phase of the star while on the bottom panel we have the plots for the Main Sequence. The region of convection is also noted on the plot.

4 Discussion

The evolution of stars is often divided into several categories, each characterized by different physical properties. In this chapter, we want to analyze these phases and discuss the physical properties as we observe them in the results we got from the simulations we contacted. The theoretical background for this analysis is provided by [7], which helps us interpret the results we got in Section 3.

4.1 Protostar

The first phase in the evolution of the star is called the protostar phase. The formation of a star begins from perturbations in an interstellar cloud causing it to collapse under its own gravity. The density increases and the gas traps radiation, which makes the star have a hydrostatic equilibrium, which slows down its collapse. At this stage the gas inside behaves as an ideal gas, as it is suggested in Figures 1 and 2.

4.2 Pre-Main Sequence

After the accretion of new material stops the star has entered the pre-main sequence phase. The cloud continues to contract due to the gravitational forces, and as a result density and temperature increase at the core. The luminosity of the cloud drops during this phase as seen in Figures 3 and 4. This is known as the Hayashi line which corresponds to the mass of the star. After that, the star starts to increase in luminosity as the core grows in mass and increases in temperature. This ends when the star is finally ready to begin thermonuclear reactions at its core. This phase is known as the zero-age main sequence. During this whole sequence, the core is still an ideal gas, while both the density and the temperature steadily increase.

As we can see in Figures 5 and 6 the way the stars transport energy during this phase is completely convective. The reason for that is the opacity of the star which is very high at this point, making it almost impossible to transmit energy with radiation.

4.3 Main-Sequence

After that, the star enters its most stable phase. During the main-sequence phase, the star burns hydrogen through thermonuclear reactions and has a hydrostatic equilibrium. Because hydrogen is converted to helium, the mean molecular weight μ increases in the core, and because $L \propto \mu^4 M^3$ with constant mass we have an increase in luminosity. This is something that we can observe in Figures 3 and 4.

The CNO cycle gives us a proportionality between the energy generation rate and the temperature $\epsilon_{CNO} \propto T^{18}$ which acts as a thermostat in the sense that it controls the temperature of the core of the star. From this relation, we can see that the central temperature of the star must increase during this phase, it is however a small increase. We can see this behavior in Figure 2. For stars with a mass lower than $1.2\,(\text{or } 1.3)\,M_\odot$ we have the pp-chain which is characterized by $\epsilon_{pp} \propto \rho T^4$. This can lead to a higher increase in both the central density and temperature of the star. This becomes clear when we compare Figure 1 to Figure 2 as we see the line that corresponds to the main sequence gets higher to bigger values of the central density.

When the energy production gets dominated by the CNO-cycle ($M > 1.2 M_\odot$) we have big amounts of energy being produced in the core that has a small mass, which leads to a convective core with a radiative envelope. This is indeed the case in Figure 6. The opposite is true for smaller masses where the pp-chain dominates and the production of the energy gets distributed over a larger area. This behavior can be seen in Figure 5.

4.4 Red Giant Branch and Horizontal Branch

Both of the stars that were simulated can be considered low-mass stars and they have the characteristic that they develop a degenerate helium core after the main sequence. This leads to a red giant branch phase that has a big duration. We can see the degenerate gas in Figures 1 and 2 after the star leaves the main sequence.

The star continues to burn hydrogen at the shells around the core, which now consists of Helium. Helium ignites when the temperature increases ($10^8 K$) in helium flashes which are unstable. We can notice these instabilities in Figures 3 and 4 as the plot goes up and down in short periods of time.

The horizontal branch is a brief period right after the helium flashes and has more stability. The core becomes once again non-degenerate as we can see in Figures 1 and 2 while the luminosity increases steadily (Figures 3 and 4).

4.5 Asymptotic Giant Branch

This phase begins when the core starts running out of helium. In the early stages the core contracts, which makes the outer layers expand, and the outer envelope starts contracting. The luminosity increases (Figures 3 and 4) and the core becomes degenerate again (Figures 1 and 2).

The next phase is the thermally pulsing Asymptotic Giant Branch (AGB), when the star reaches the H-He discontinuity. This phase is more evident in the higher mass star, where we can see the pulses in Figure 4.

Both stars leave the AGB phase with the loss of the outer layers with a weak but fast wind. In the H-R diagrams (Figures 3 and 4) we can see the characteristic horizontal line of this phase as the temperature increases while the luminosity remains constant. During this phase, the core becomes extremely relativistic (Figures 1 and 2), thus creating a White Dwarf.

4.6 White Dwarf

In this phase, the core of the star is extremely relativistic as it is indicated in Figures 1 and 2. The star has lost all the envelope and there are no nuclear reactions. As a result, the luminosity is provided by radiating the remaining thermal energy that is stored in the star. The star is cooling at an almost constant radius and the luminosity rapidly decreases. We can see this behavior in Figures 3 and 4.

5 Conclusion

We modeled the evolution of two stars with masses 1, 2 $M_\odot$ to study the different phases they undergo until they become a white dwarf. We were interested in studying the evolution in the $\log(T_c) - \log(\rho_c)$ plane where we can note many interesting properties of these phases, and also in the H-R diagram where we can see the observable properties of the stars. We also studied how these stars transmit energy in their different layers at the pre-main and main sequence. The analysis of these plots with the theory of star evolution [7] has shown the similarities and differences in the evolution of these two stars with different values of mass.

References

[1] Bill Paxton et al. "Modules for Experiments in Stellar Astrophysics (MESA)". In: 192.1, 3 (Jan. 2011), p. 3. DOI: 10.1088/0067-0049/192/1/3. arXiv: 1009.1622 [astro-ph.SR].

[2] Bill Paxton et al. "Modules for Experiments in Stellar Astrophysics (MESA): Planets, Oscillations, Rotation, and Massive Stars". In: 208.1, 4 (Sept. 2013), p. 4. DOI: 10.1088/0067-0049/208/1/4. arXiv: 1301.0319 [astro-ph.SR].

[3] Bill Paxton et al. "Modules for Experiments in Stellar Astrophysics (MESA): Binaries, Pulsations, and Explosions". In: 220.1, 15 (Sept. 2015), p. 15. DOI: 10.1088/0067-0049/220/1/15. arXiv: 1506.03146 [astro-ph.SR].

[4] Bill Paxton et al. "Modules for Experiments in Stellar Astrophysics (MESA): Pulsating Variable Stars, Rotation, Convective Boundaries, and Energy Conservation". In: 243.1, 10 (July 2019), p. 10. DOI: 10.3847/1538-4365/ab2241. arXiv: 1903.01426 [astro-ph.SR].

[5] Adam S. Jermyn et al. "Modules for Experiments in Stellar Astrophysics (MESA): Time-dependent Convection, Energy Conservation, Automatic Differentiation, and Infrastructure". In: 265.1, 15 (Mar. 2023), p. 15. DOI: 10.3847/1538-4365/acae8d. arXiv: 2208.03651 [astro-ph.SR].

[6] Bill Wolf. *PyMesaReader*. https://github.com/wmwolf/py_mesa_reader. 2022.

[7] Onno Pols. *Stellar structure and evolution*. https://www.astro.ru.nl/~onnop/education/stev_utrecht_notes/. 2011.